WISCONSIN
INDIANA
YALE
NOAO

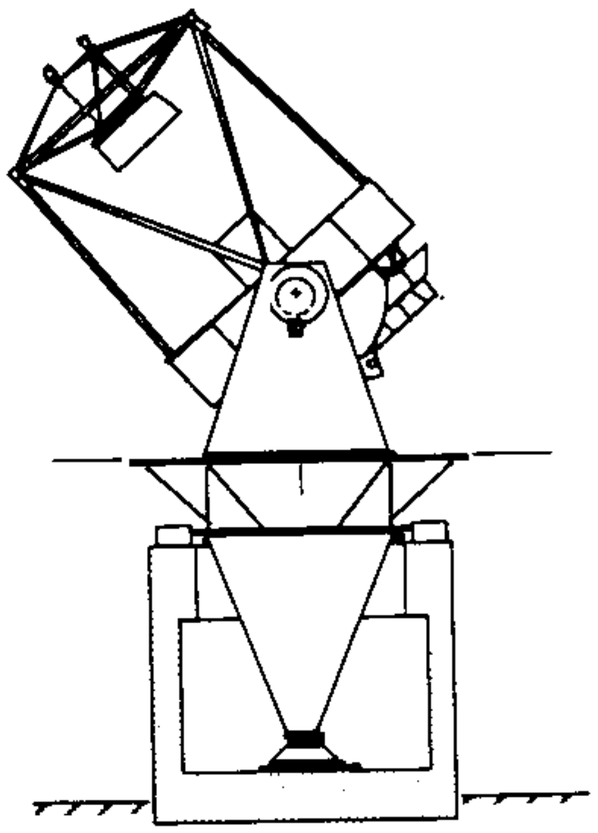

3.5 METER TELESCOPE

Altitude and Elevation Servo Analysis for the WIYN 3.5 Meter Telescope

J. Alan Schier

The Observatories
of the
Carnegie Institution of Washington
Pasadena, California

WODC 02-10-01

6/26/91

MAIN DRIVE SERVO ANALYSIS AND DESIGN

The servo analysis and design for the main drives primarily addresses the following three issues: 1. Rejection of drive motor ripple torques; 2. Accurate following of command inputs; 3. Good transient response to command inputs. In all three of these areas, good results are achieved with controllers that are robust and relatively uncomplicated.

Figure 1 shows a block diagram of the generic system that was applied to both the altitude and azimuth axis. The servo design includes both the compensator and the prefilter, with the compensator governing primarily the ripple rejection and command following performance, and the prefilter governing the input transient performance.

The design for both axes followed the same path. It began with the data from the finite element frequency response analysis (FRA) from which a model was built for servo design purposes (FRA results and the accompanying model are presented in the section covering the finite element analysis). This frequency response was then modified by the addition of the compensator. The results of this step are shown in Figure 2a,b for the altitude axis and Figure 3a,b for the azimuth axis. The major features are the 4 Hz and 6 Hz crossover frequencies for the altitude and azimuth axes respectively, and a 50 degree phase margin in both cases. In both cases, the gain margin is also large (greater than 10) indicating that the system will be insensitive to any reasonable parameter variations.

Figures 4 and 5 show the closed-loop motor ripple disturbance transmission for the altitude and azimuth axes respectively. In both cases, the peak errors are under 10 milliarcseconds. These errors are small enough that they will largely be masked by the resolution of the encoders. Figures 6 shows the command following error for the azimuth axis for a trajectory that passes near zenith. For practical purposes, the error is zero. The small amount of variation evident is numerical noise from the computational algorithm.

Finally Figures 7 and 8 show the small-signal (less than 10 arcsecond) step responses of the altitude and azimuth axes both with and without a prefilter. In both cases without a prefilter there is a large overshoot and a long settling time. With the prefilter, the overshoot is limited to about 5% and despite the slower risetime, the settling time is near optimal.

The servo design equations are given in the appendix. Both compensators are second-order equations and both prefilters are fourth-order. When implemented digitally, these computations should be well within the capabilities of modest digital hardware.

A Note on the FRA Data

The data generated by the FRA processor for the azimuth axis shows a frequency response that does not quite agree with an analytical check done by hand. The FRA data shows a magnitude response that is uniformly high by a factor of 3.25. In other words, the FRA says that the azimuth response to an input is 3.25 times larger than the analytical check predicts.

We have not yet been able to resolve this difference, but have proceeded along the conservative route by using the FRA data. This has the effect of making the disturbance rejection of the overall system approximately 3.25 times worse than otherwise. Within this assumption, we have been able to design a servo that is not overly complicated and performs quite well.

If the analytical check turns out to be in fact correct, the same basic servo can be used and will show even better performance. This would require only a minor change in the servo software.

For the altitude axis, the data generated by the FRA processor is consistent with an analytical check of the overall magnitude. In this case, we expect the performance of the physical system to be very nearly the same as the analytical model.

WIYN ALTITUDE AXIS SERVO DESIGN

Altitude axis model:

$$H = \frac{\Theta}{T} = \frac{(2.771\times10^{-5})(s+.294\pm j31.953)(s+.314\pm j29.528)(s+.248\pm j23.581)(.0914\pm j8.78)}{(2\pi)^2(s^2)(s+.3874\pm j32.894)(s+.323\pm j31.12)(s+.254\pm j25.482)(s+.0979\pm j9.604)}$$

Closed loop compensator:

$$G = \frac{T}{E} = \frac{(s+.5333\pm j1.333)(1.367\times10^{8})}{s(s+12)}$$

Prefilter

$$P = \frac{\Theta'_c}{\Theta_c} = \frac{(288.4)(s+.35\pm j1.55)}{(2\pi)^2(s+2.121\pm j2.121)(s+.530\pm j1.33)}$$

Ripple frequency = 97 $\frac{\text{cycles}}{\text{rev}}$ at motor

Drive ratio = 30

Ripple amplitude = 37 N m

WIYN AZIMUTH AXIS SERVO DESIGN

Azimuth axis model:

$$H = \frac{\Theta}{T} = \frac{(2.0527\times10^{-3})(s+.3325\pm j33.25)(s+.2402\pm j24.02)}{(2\Pi)^2(s^2)(s+.3346\pm j33.46)(s+.254\pm j25.4)}$$

Closed loop compensator:

$$G = \frac{T}{E} = \frac{(1.9191\times10^{8})(s+0.8\pm j2)}{s(s+18)}$$

Prefilter:

$$P = \frac{\Theta'_c}{\Theta_c}\,\frac{(.12957)(s+8.316\pm j5.63)(s+.51\pm j2.328)}{(s+2.828\pm j2.828)(s+0.8\pm j2)}$$

Ripple Frequency = 97 $\frac{\text{cycles}}{\text{rev}}$ at motor

Drive Ratio = 35

Ripple Amplitude = 37 N m

Note: The transfer functions in this appendix are presented in a form that may be unfamiliar. In these equations, we use

$$s=j2(pi)f,$$

where

j=the imaginary unit (sqrt(-1)),
f=frequency in Hertz.

This allows the pole and zero positions to be seen directly in the factors of the transfer function.

In contrast, transfer functions are frequently presented using

$$s=jw,$$

where

w=frequency in radians/sec.

When done in this manner, the pole and zero positions are evident only in terms of radians/sec which most people mentally convert to Hertz anyway.

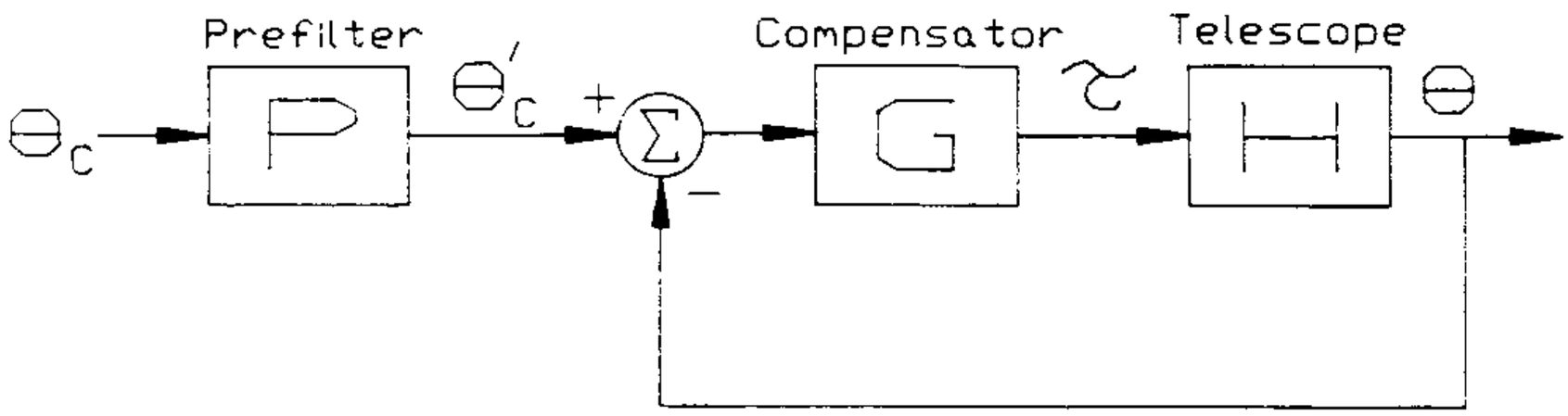

Figure 1. System Block Diagram. This figure is a block diagram model of either axis of the main servos. The prefilter block takes as its input a commanded angle and outputs a filtered version of that command. The compensator has as its input the error signal that is the difference between the filtered command and the actual position of the telescope (as measured by the encoder). The output of the compensator is a torque which acts on the telescope dynamics. The telescope responds to this torque with the angle that is measured by the encoder.

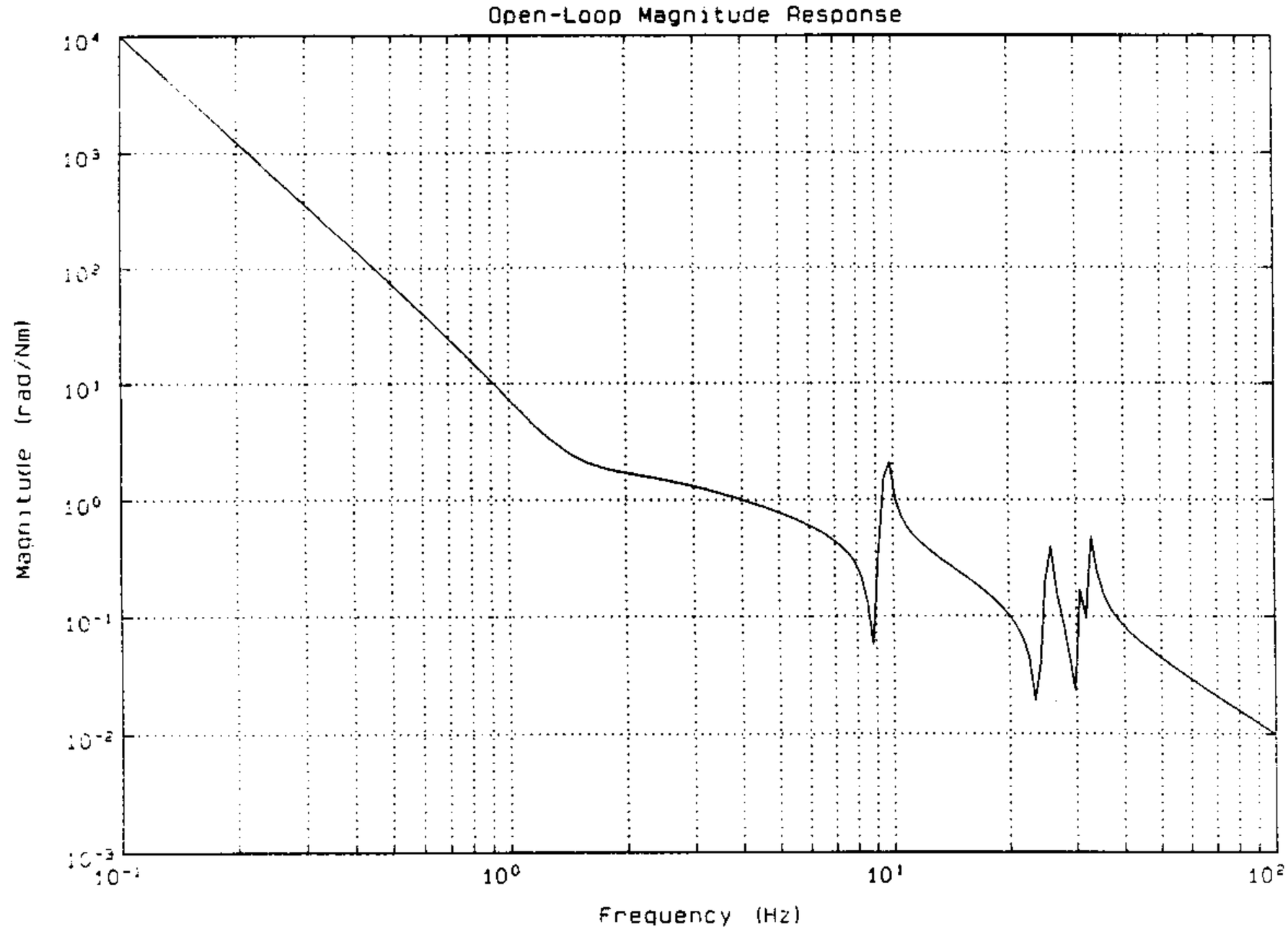

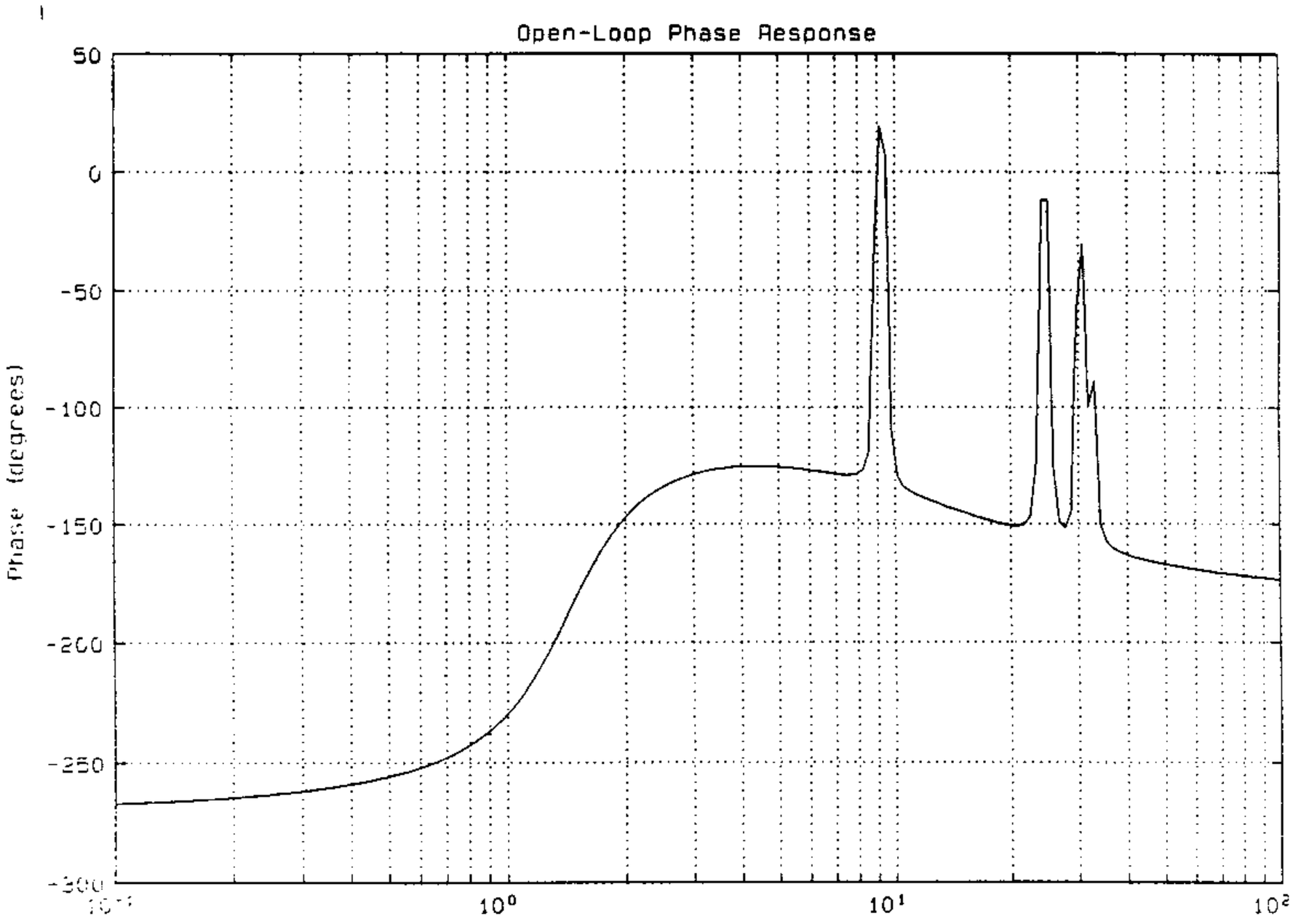

Figure 2a,b. **<u>Altitude Axis Open-loop Magnitude and Phase Response.</u>** **With the compensator in the loop, the magnitude plot shows a crossover frequency of 4 Hz, and the phase plot shows a phase margin of about 50 degrees. These results assume a ripple frequency of 97 cycles/revolution and an amplitude of 37 Nm measured at the motor. The assumed drive ratio is 30.**

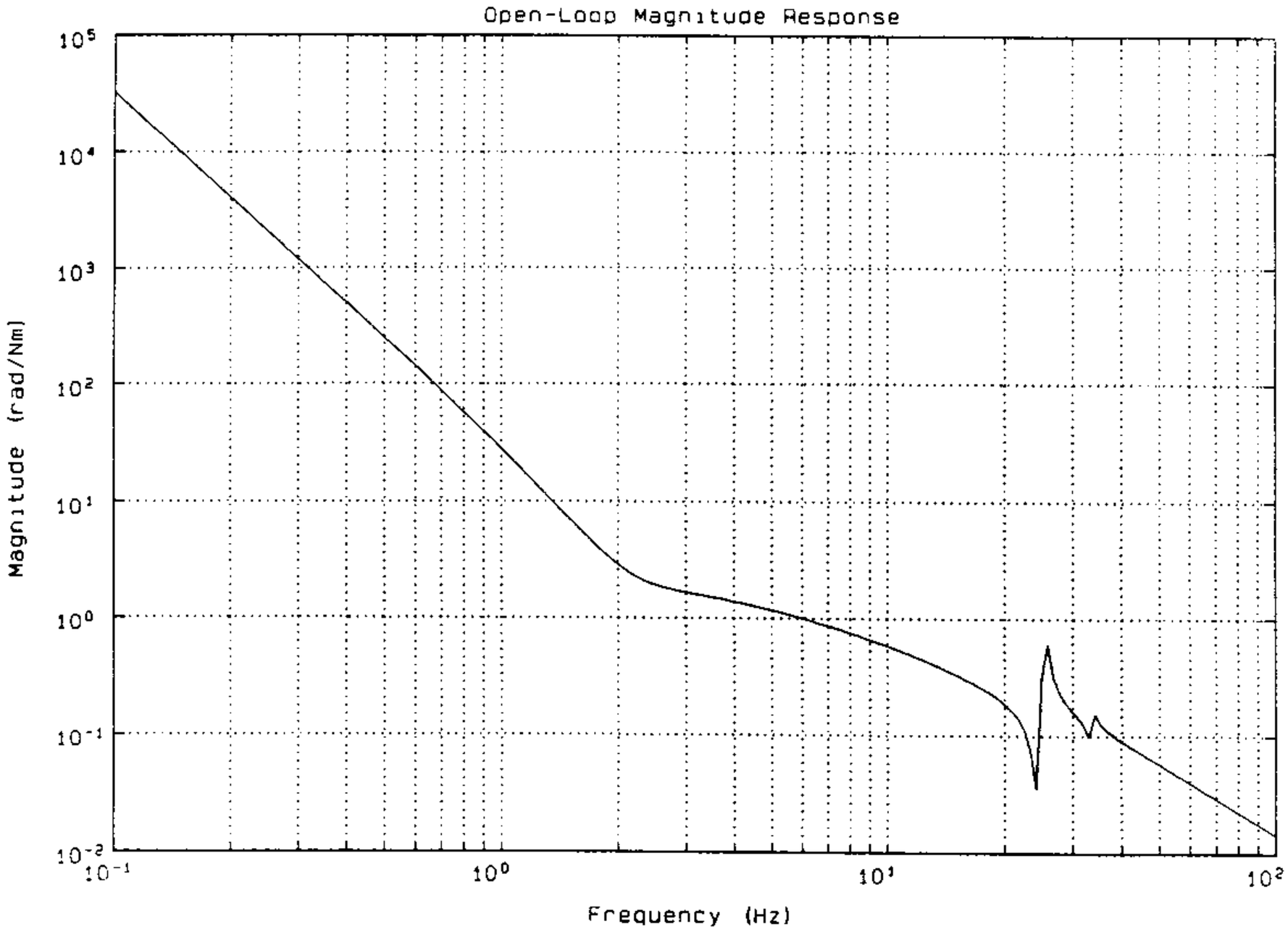

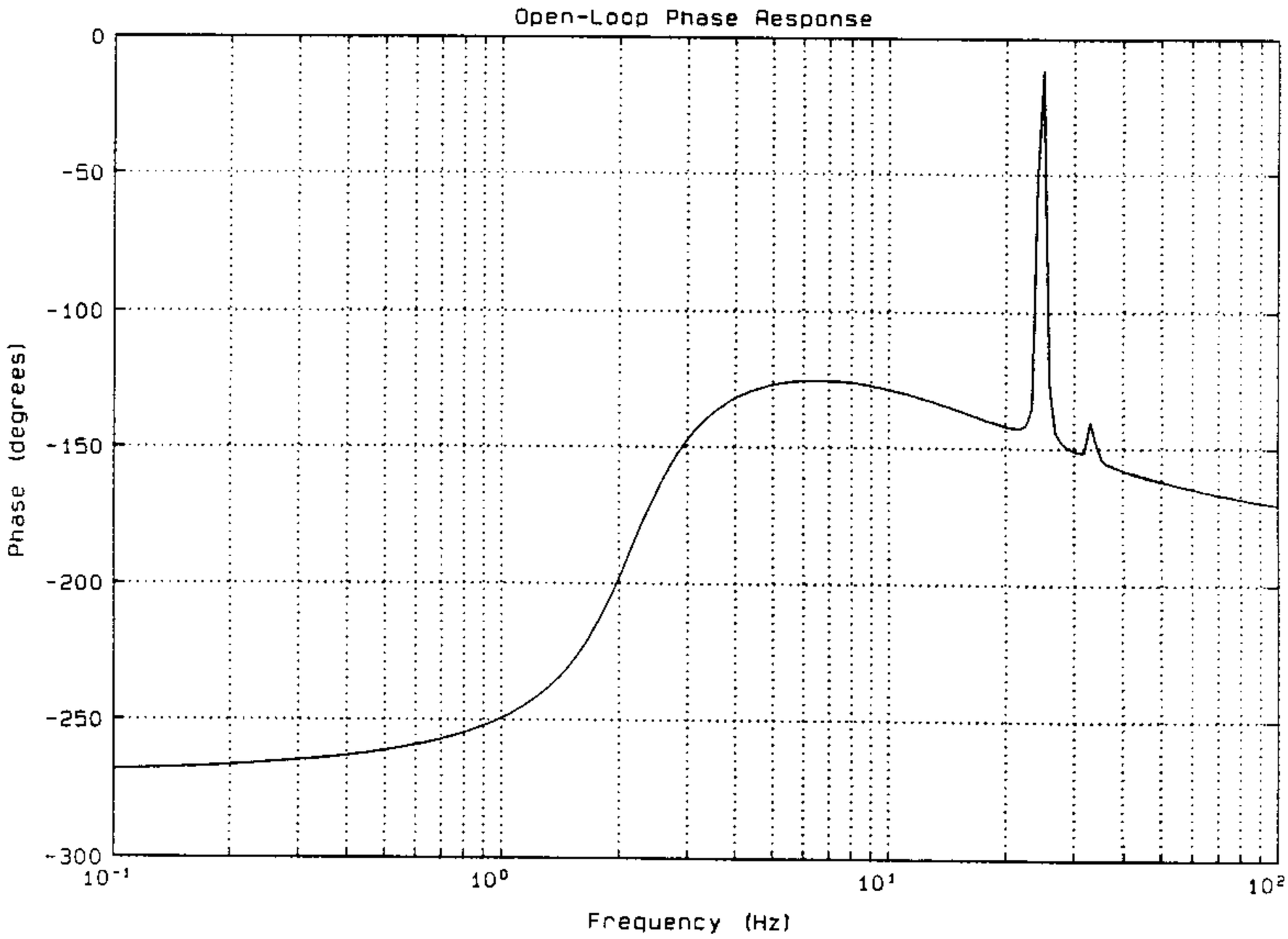

Figure 3a,b. **Azimuth Axis Open-loop Magnitude and Phase Response.** With the compensator in the loop, the magnitude plot shows a crossover frequency of 6 Hz, and the phase plot shows a phase margin of about 50 degrees. These results assume a ripple frequency of 97 cycles/revolution and an amplitude of 37 Nm measured at the motor. The assumed drive ratio is 35

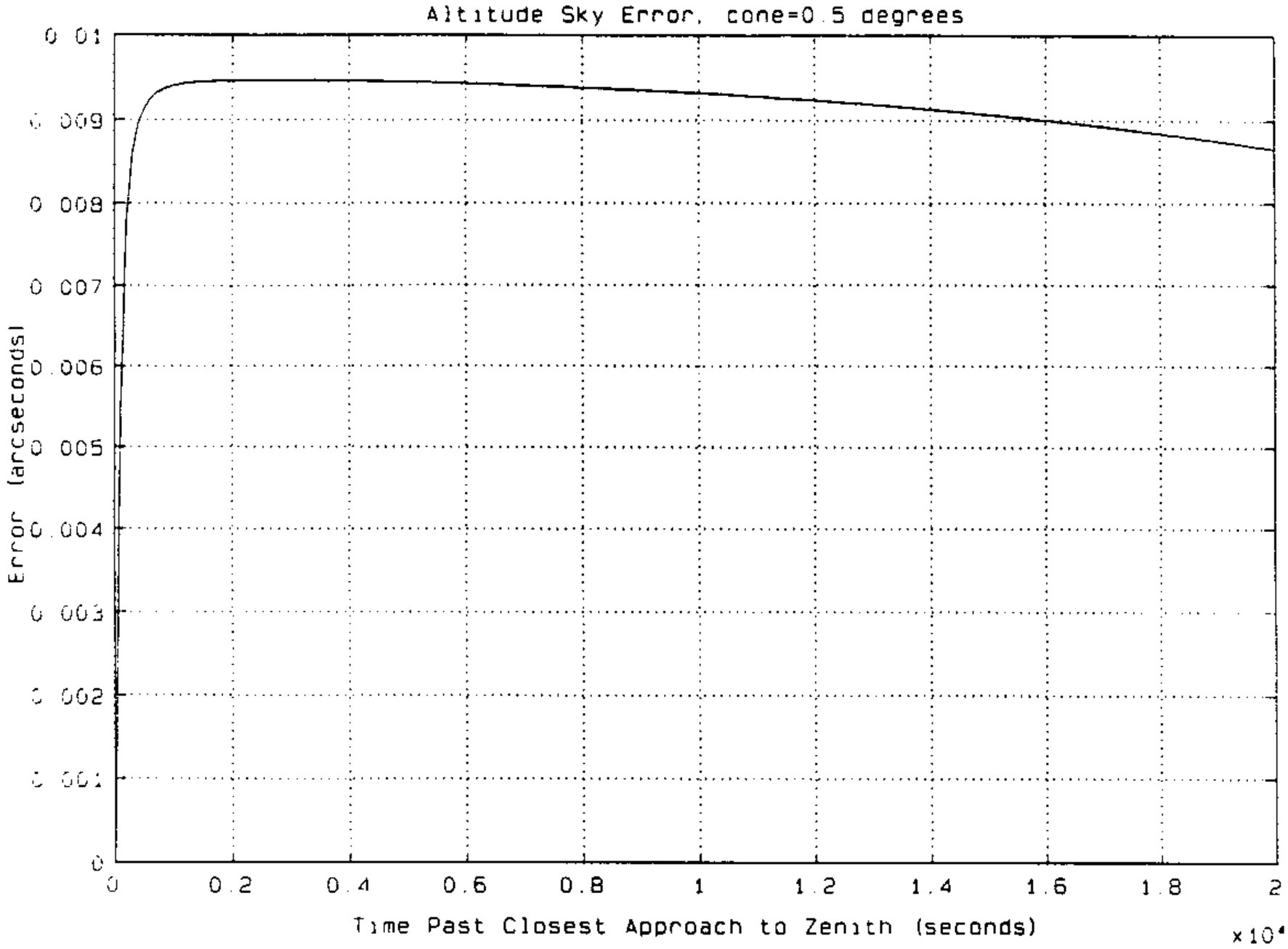

Figure 4. <u>Altitude Axis Ripple Transmission.</u> This plot shows the altitude error due to motor ripple torque which is seen to stay below 10 milliarcseconds. These results are for a trajectory that passes within 0.5 degrees of zenith.

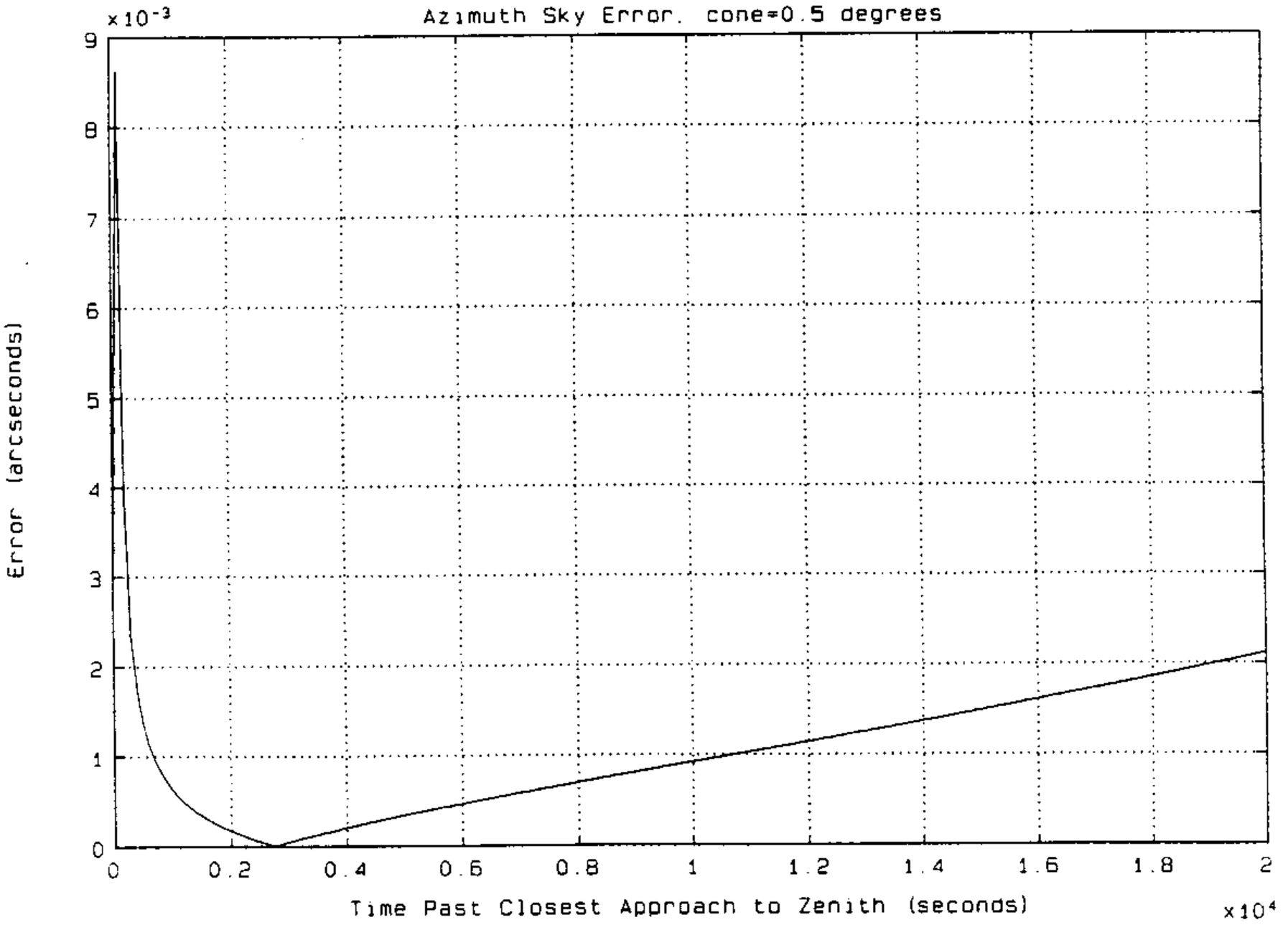

Figure 5. <u>Azimuth Axis Ripple Transmission.</u> This plot shows the azimuth error projected onto the sky due to motor ripple torque which is seen to stay below 9 milliarcseconds. These results are for a trajectory that passes within 0.5 degrees of zenith.

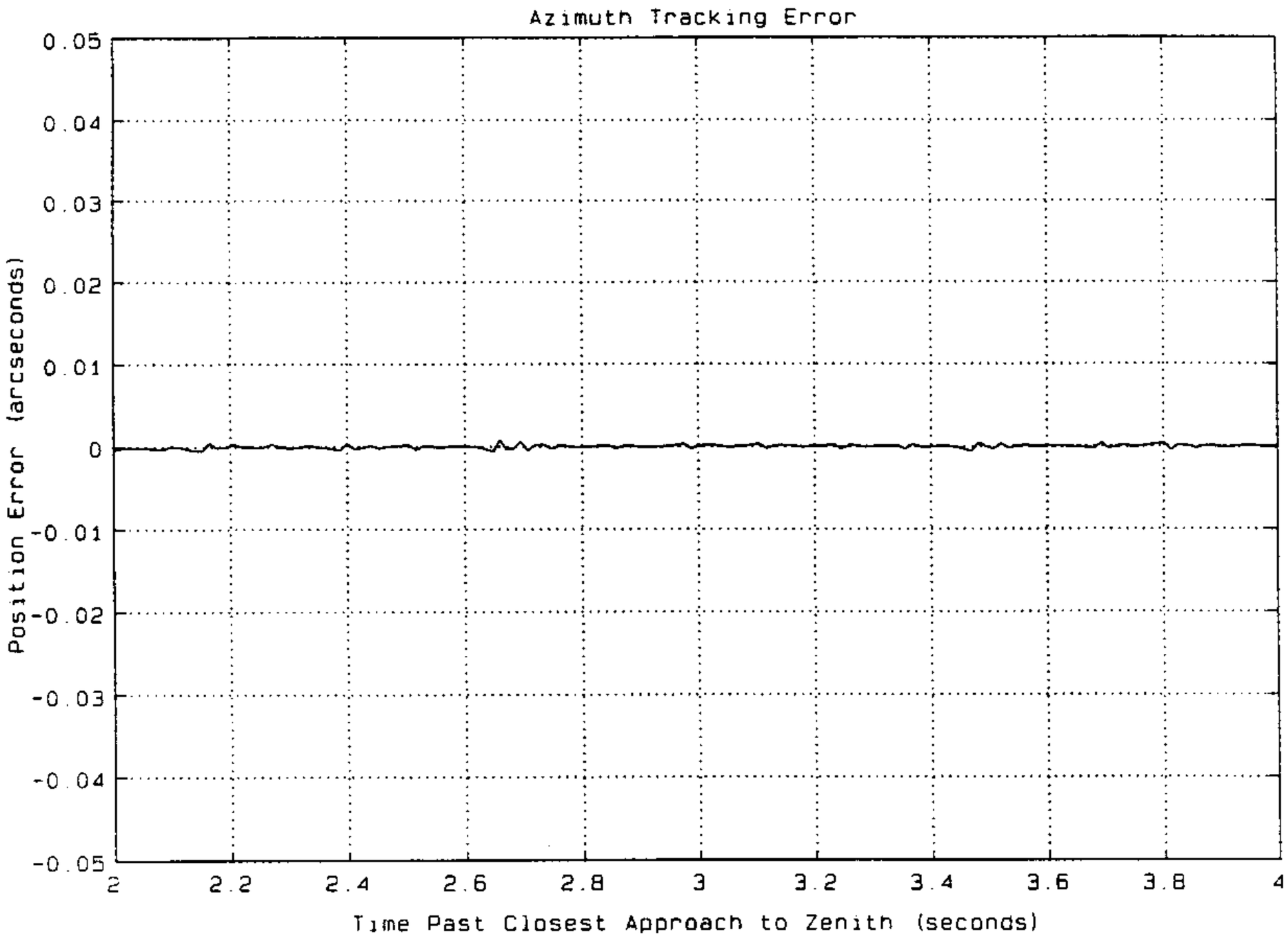

Figure 6. <u>Azimuth Axis Command Following Error.</u> This plot shows the command following error in the azimuth axis during a time of near maximum tracking rate (near zenith). The error is practically zero.

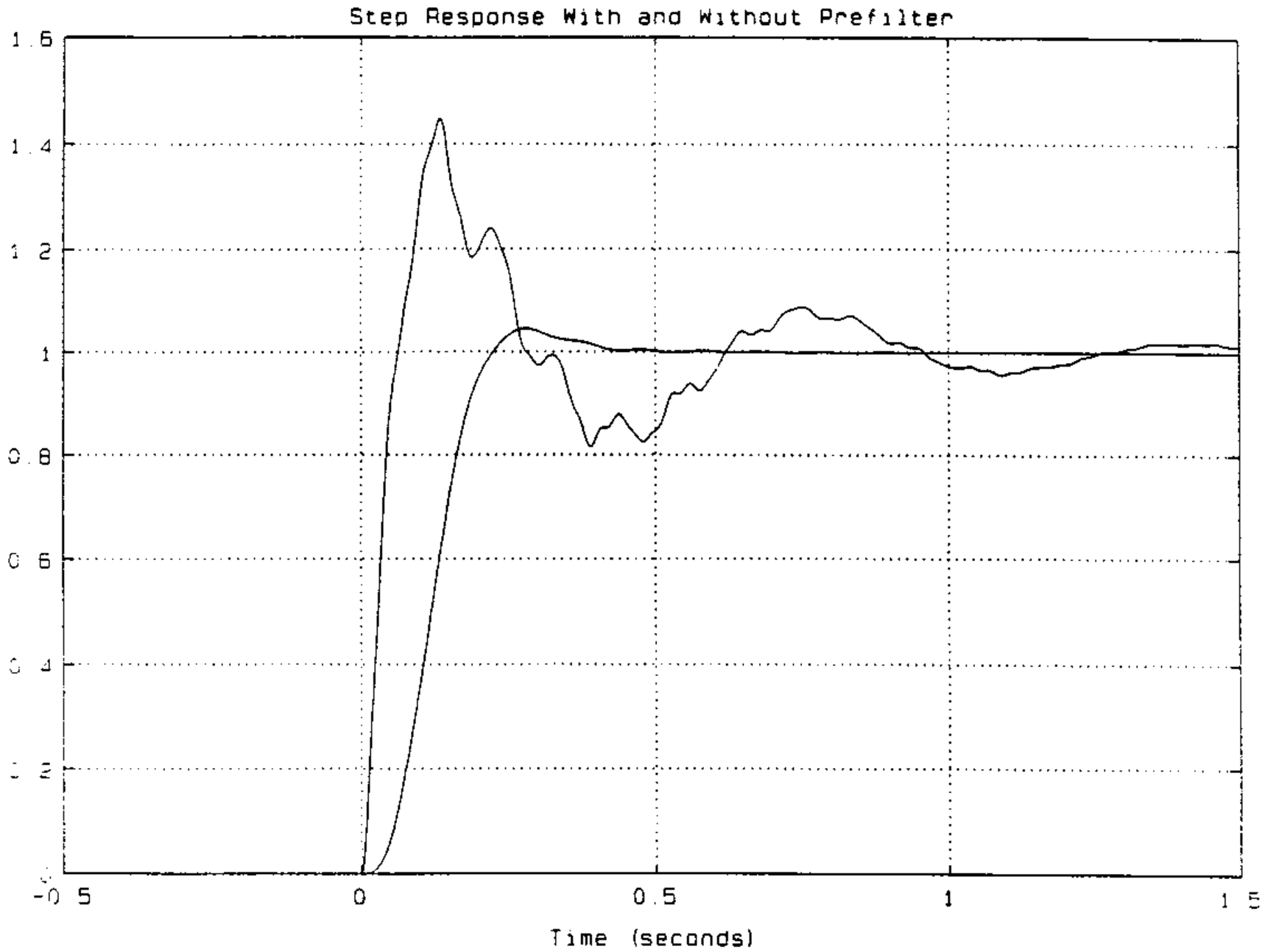

Figure 7. Altitude Closed-loop Step Response. This plot shows the response of the altitude axis to a step input both with and without a prefilter. The fast-rising response with about 35% overshoot corresponds to the system without the prefilter. The slower rising response with the prefilter in the system shows about 5% overshoot and settles much sooner. The excitation of the mode near 25 Hz is also considerably less with the prefilter.

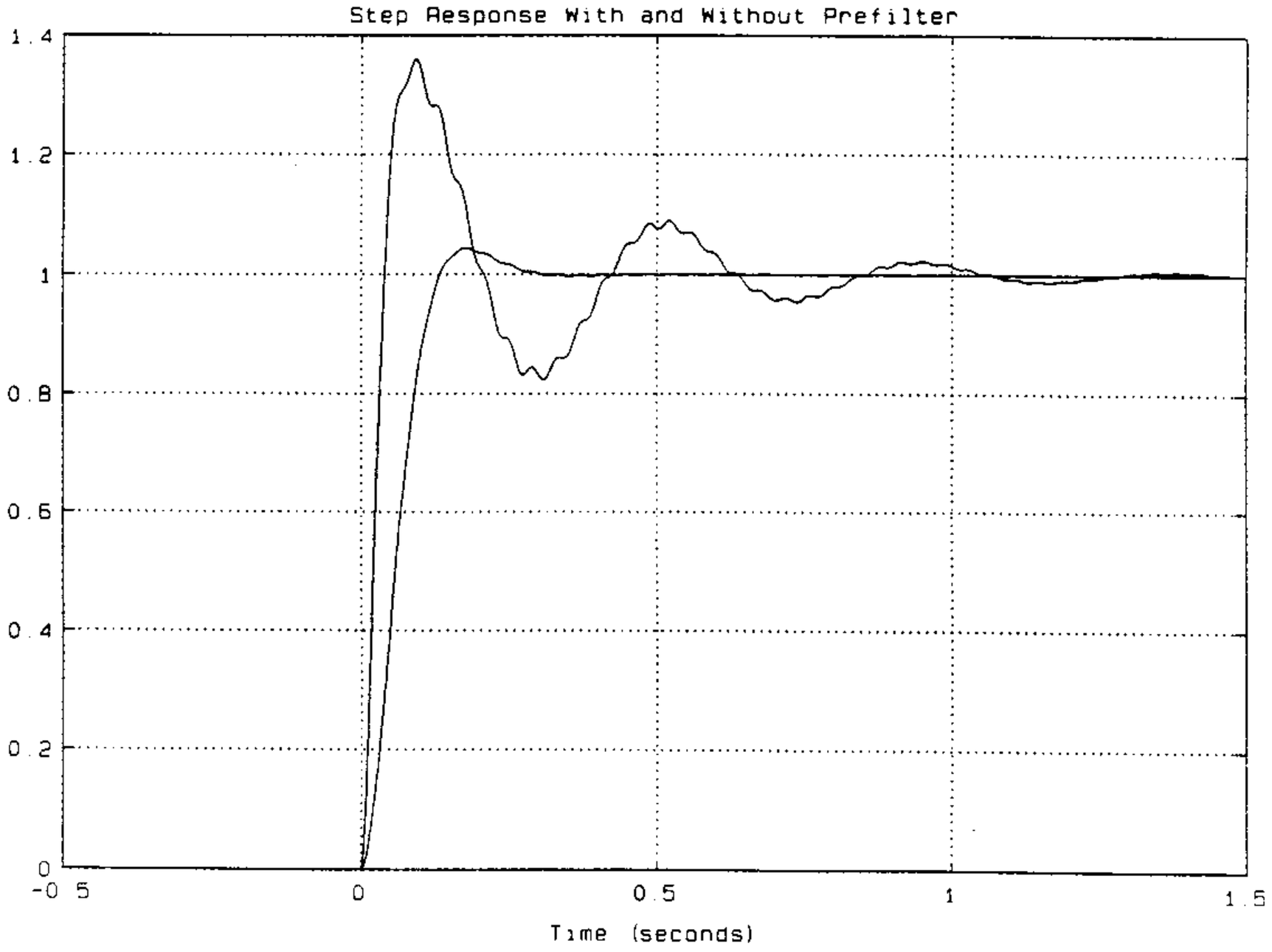

Figure 8. Azimuth Closed-loop Step Response. This plot shows the response of the azimuth axis to a step input both with and without a prefilter. The fast-rising response with a large overshoot corresponds to the system without a prefilter. The slower rising response with the prefilter shows about 5% overshoot and settles much sooner.